

## Chemical and Cytotoxic Constituents from the Leaves of *Cinnamomum kotoense*

Ching-Hsein Chen,<sup>†</sup> Wen-Li Lo,<sup>‡</sup> Ya-Chen Liu,<sup>†</sup> and Chung-Yi Chen<sup>\*‡</sup>

Graduate Institute of Biopharmaceutics, College of Life Sciences, National Chiayi University, Chiayi 600, Taiwan, Republic of China, and Basic Medical Science Education Center, Fooyin University, Kaohsiung County 831, Taiwan, Republic of China

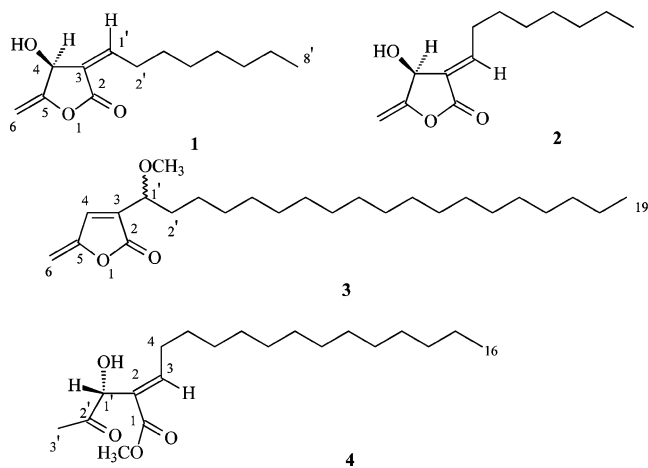
Received March 14, 2006

Three new butanolides, kotomolide A (**1**), isokotomolide A (**2**), and kotomolide B (**3**), and a new secobutanolide, secokotomolide A (**4**), along with 21 known compounds were isolated from the leaves of *Cinnamomum kotoense*. Their structures were determined by spectroscopic analyses. Compound **4** was found to induce significant cell death in the human HeLa cell line. Apoptotic-related DNA damage can be positively related to the dose of compound **4**. The DNA damage was measured by the percentage of subG1 (24 h after the treatment of compound **4**) as determined by cell cycle analysis and TUNEL assay. Treatment with **4** significantly increased intracellular H<sub>2</sub>O<sub>2</sub> and/or peroxide, nitric oxide (NO) at 1, 3, and 24 h. Our results also showed that compound **4** induced (a) noticeable reduction of mitochondrial transmembrane potential ( $\Delta\Psi_m$ ), (b) activation of caspase 3/7, and (c) up-regulation of the p53 expression. Compound **4**-induced DNA damage was found to markedly decrease when the cells were pretreated with an intracellular glutathione supplement (glutathione ethyl ester). These results suggest that an increase of H<sub>2</sub>O<sub>2</sub> and/or peroxide by compound **4** is the initial apoptotic event. The intracellular GSH depletion is a critical event in compound **4**-induced apoptosis in HeLa cells.

*Cinnamomum kotoense* Kanehira & Sasaki (Lauraceae) is a small evergreen tree, endemic to Lanyu Island of Taiwan, and has recently been cultivated as an ornamental plant.<sup>1</sup> There are only two papers describing the constituents of this species.<sup>2,3</sup> In continuation of a program toward the studies of chemotaxonomy and biologically active metabolites from Formosan Lauraceous plants, an MeOH extract of the leaves of *C. kotoense* afforded three new butanolides, kotomolide A [(4*S*,3*Z*)-4-hydroxy-5-methylene-3-octylenedihydrofuran-2-one] (**1**), isokotomolide A [(4*S*,3*E*)-4-hydroxy-5-methylene-3-octylenedihydrofuran-2-one] (**2**), and kotomolide B [3-(1-methoxynonadecyl)-5-methylene-5*H*-furan-2-one] (**3**), a new secobutanolide, secokotomolide A {methyl[(2*E*)-2-[(1*R*)-1-hydroxy-2-oxopropyl]hexadec-2-enoate]} (**4**), and 21 known compounds, including two butanolides, obtusilactone A<sup>4</sup> and isoobtusilactone A,<sup>4</sup> three flavan-3-ols, (+)-catechin,<sup>5</sup> (–)-catechin,<sup>6</sup> and (–)-epicatechin,<sup>7</sup> four lignans, (–)-sesamin,<sup>8</sup> (+)-syringaresinol,<sup>9</sup> pluviatilol,<sup>10</sup> and clemaphenol A,<sup>11</sup> six benzenoids, isoeugenol,<sup>12</sup> vanillin,<sup>13</sup> vanillic acid,<sup>14</sup> ferulic acid,<sup>15</sup> *p*-hydroxybenzaldehyde,<sup>16</sup> and syringaldehyde,<sup>17</sup> four steroids,  $\beta$ -sitosterol,<sup>18</sup> stigmasterol,<sup>18</sup>  $\beta$ -sitosteryl-D-glucoside,<sup>19</sup> and stigmasteryl-D-glucoside,<sup>19</sup> and two aliphatic compounds, palmitic acid<sup>20</sup> and stearic acid.<sup>21</sup> In this paper, we report the structural elucidation of **1–4** and the apoptotic inducing capability of secokotomolide A (**4**) on a human cervical cancer cell line, HeLa.

### Results and Discussion

Kotomolide A (**1**) was isolated as a pale yellowish liquid. Its molecular formula, C<sub>13</sub>H<sub>20</sub>O<sub>3</sub>, was established by HRFABMS. The UV absorption at 228 nm was similar to that of obtusilactone A,<sup>4</sup> indicating the presence of  $\beta$ -hydroxy- $\gamma$ -methylene- $\alpha,\beta$ -unsaturated- $\gamma$ -lactone.<sup>22</sup> The IR spectrum showed absorption bands for a hydroxy group at 3450 cm<sup>-1</sup> and an  $\alpha,\beta$ -unsaturated  $\gamma$ -lactone moiety at 1768 and 1680 cm<sup>-1</sup>. The <sup>1</sup>H NMR spectrum of **1** was similar to that of obtusilactone A,<sup>4</sup> indicating that **1** has the same  $\beta$ -hydroxy- $\gamma$ -methylene- $\alpha,\beta$ -unsaturated- $\gamma$ -lactone skeleton and the same *Z* geometry of the trisubstituted double bond [ $\delta$  6.63 (1H, td, *J* = 7.9, 2.1 Hz, H-1')]. The presence of a broad singlet at  $\delta$  1.29



(8H, br s, H-4'–7') was attributed to protons in an aliphatic chain in **1**. The exocyclic olefinic protons appeared at  $\delta$  4.57 and 4.72 (each 1H, dd, *J* = 2.8, 1.5 Hz, H-6a, b), and one hydroxymethine proton was located at  $\delta$  5.16 (1H, br s, H-4). Compound **1** showed an  $[\alpha]_D^{25} -43.2$  (*c* 0.023, CHCl<sub>3</sub>), indicating the *S* configuration at C-4.<sup>23</sup> Thus, the structure of kotomolide A was represented as **1** and elucidated as (4*S*,3*Z*)-4-hydroxy-5-methylene-3-octylenedihydrofuran-2-one.

Isokotomolide A (**2**), a pale yellowish liquid, also had the molecular formula C<sub>13</sub>H<sub>20</sub>O<sub>3</sub>, as deduced from HRFABMS. Its spectroscopic data (IR, UV, <sup>1</sup>H and <sup>13</sup>C NMR) were similar to those of **1**. A large difference involves H-1',  $\delta$  6.93 (td, *J* = 7.9, 2.1 Hz) in **2** versus  $\delta$  6.63 in **1**, suggesting an *E* configuration for  $\Delta^{3(1)}$  in **2**. The <sup>1</sup>H NMR spectrum of **2** was similar to that of isoobtusilactone A,<sup>4</sup> indicating that **2** has the same  $\beta$ -hydroxy- $\gamma$ -methylene- $\alpha,\beta$ -unsaturated- $\gamma$ -lactone skeleton and the same *E* geometry of the trisubstituted double bond [ $\delta$  6.93 (1H, td, *J* = 7.9, 2.1 Hz, H-1')]. The presence of a broad singlet,  $\delta$  1.27 (8H, br s, H-4'–7'), was attributed to protons in an aliphatic chain in **2**. The exocyclic olefinic protons appeared at  $\delta$  4.63 and 4.78 (each 1H, dd, *J* = 2.8, 1.5 Hz, H-6a,b), and one hydroxymethine proton was located at  $\delta$  5.32 (1H, br s, H-4). Compound **2** showed an  $[\alpha]_D^{25} -45.6$  (*c* 0.75, CHCl<sub>3</sub>), indicating the *S* configuration at C-4.<sup>24</sup> Thus, the structure of isokotomolide A was represented as **2** and elucidated as (4*S*,3*E*)-4-hydroxy-5-methylene-3-octylenedihydrofuran-2-one. The <sup>1</sup>H

\* Corresponding author. Fax: +886-7-7834548. E-mail: xx377@mail.fy.edu.tw.

<sup>†</sup> National Chiayi University.

<sup>‡</sup> Basic Medical Science Education Center, Fooyin University.

**Table 1.**  $^1\text{H}$  NMR Data of Butanolides **1** and **2** (500 MHz,  $\delta$  in ppm,  $J$  in Hz, acetone- $d_6$ )

proton	kotomolide A ( <b>1</b> )	isokotomolide A ( <b>2</b> )
4	5.16 (1H, br s)	5.32 (1H, br s)
6a	4.57 (1H, dd, $J = 2.8, 1.5$ )	4.63 (1H, dd, $J = 2.8, 1.5$ )
6b	4.72 (1H, dd, $J = 2.8, 1.5$ )	4.78 (1H, dd, $J = 2.8, 1.5$ )
1'	6.63 (1H, td, $J = 7.9, 2.1$ )	6.93 (1H, td, $J = 7.9, 2.1$ )
2'	2.73 (2H, m)	2.47 (2H, m)
3'	1.50 (2H, m)	1.54 (2H, m)
4'-7'	1.29 (8H, br s)	1.27 (8H, br s)
8'	0.87 (3H, t, $J = 7.0$ )	0.87 (3H, t, $J = 7.0$ )
OH-4	2.08 (1H, br s, $J = 7.6$ )	2.08 (1H, br s, $J = 7.6$ )

**Table 2.**  $^{13}\text{C}$  NMR Data of Butanolides **1** and **2** (125 MHz,  $\delta$  in ppm, acetone- $d_6$ )

proton	kotomolide A ( <b>1</b> )	isokotomolide A ( <b>2</b> )
2	166.1 (s)	167.3 (s)
3	128.7 (s)	129.3 (s)
4	69.1 (d)	66.6 (d)
5	159.7 (s)	159.9 (s)
6	88.9 (t)	90.0 (t)
1'	149.6 (d)	148.5 (d)
2'-5'	28.6-29.9 (t)	29.6-30.4 (t)
6'	34.3 (t)	32.7 (t)
7'	23.4 (t)	23.4 (t)
8'	14.4 (q)	14.4 (q)

and  $^{13}\text{C}$  NMR data of **2** were assigned by comparison with those of **1** (Tables 1 and 2).

Kotomolide B (**3**) was isolated as a colorless oil. The molecular formula was determined as  $\text{C}_{25}\text{H}_{44}\text{O}_3$  by EIMS ( $[\text{M}]^+$ ,  $m/z$  392) and HREIMS. The presence of an  $\alpha,\beta$ -unsaturated  $\gamma$ -lactone moiety was apparent from a UV absorption at 265 nm.<sup>25</sup> The IR spectrum showed an  $\alpha,\beta$ -unsaturated  $\gamma$ -lactone at 1780 and 1680  $\text{cm}^{-1}$ . The  $^1\text{H}$  NMR spectra of **3** exhibited the presence, respectively, of an exomethylene group at  $\delta$  4.88 (1H, d,  $J = 2.6$  Hz) and at 5.20 (1H, d,  $J = 2.6$  Hz), as well as an olefinic proton at  $\delta$  7.22 (1H, br s). Also, it showed the signals corresponding to a methoxy functionality at  $\delta$  3.35 (3H, s), an oxymethine proton at  $\delta$  4.12 (1H, dd,  $J = 7.4, 4.8$  Hz), and long-chain aliphatic protons at  $\delta$  1.26 (30H, br s) and 1.42-1.68 (4H, m). The structure of **3** was similar to those of the known butanolide 3-(1-methoxyoctadecyl)-5-methylene-5H-furan-2-one.<sup>22</sup> Thus, the structure of **3** was elucidated as 3-(1-methoxynonadecyl)-5-methylene-5H-furan-2-one. Compound **3** has a negative specific rotation, but the configuration at C-1' remains undefined.

Secokotomolide A (**4**), a pale yellowish liquid, also had the molecular formula  $\text{C}_{20}\text{H}_{36}\text{O}_4$ , as deduced from HRFABMS. The UV absorption at 215 nm was similar to that of secolincomolide A,<sup>26</sup> indicating the presence of a secobutanolide skeleton.<sup>26</sup> The IR spectrum of **4** showed characteristic absorption bands due to the presence of hydroxyl (3450  $\text{cm}^{-1}$ ), ester (1735  $\text{cm}^{-1}$ ), and ketone (1710  $\text{cm}^{-1}$ ) groups. The  $^1\text{H}$  NMR spectrum of **4** was similar to that of secomahubanolide,<sup>22</sup> except for the *E* geometry of the trisubstituted double bond [ $\delta$  6.98 (1H, t,  $J = 7.6$  Hz, H-3)] in **4** instead of the *Z* geometry [ $\delta$  6.34 (1H, t,  $J = 7.6$  Hz, H-3)] in secomahubanolide.<sup>22</sup> Secomahubanolide showed four more methylene units [ $\delta$  1.27 (28H, br s, H-6-19)] than secokotomolide A (**4**) [ $\delta$  1.28 (20H, br s, H-6-15)] in the side chain. An acetyl and one *O*-methyl group were observed at  $\delta$  2.12 (3H, s, H-3') and 3.65 (3H, s, OMe-1), respectively. Compound **4** showed negative specific rotation  $\{[\alpha]^{25}_{\text{D}} -52.1 (c 0.15, \text{CHCl}_3)\}$ , indicating the 1'*R* configuration similar to that of secomahubanolide  $\{[\alpha]^{25}_{\text{D}} -11.2 (c 0.029, \text{CHCl}_3)\}$ ,<sup>22</sup> but contrary to that of secoisolanCIFolide  $\{[\alpha]^{25}_{\text{D}} +102.7 (c 0.49, \text{CHCl}_3)\}$ .<sup>25</sup> From the above data, compound **4** was defined as methyl[(2*E*)-2-[(1*R*)-1-hydroxy-2-oxopropyl]-hexadec-2-enoate].

To evaluate the anticancer effects of secokotomolide A (**4**), we first examined whether the induction of apoptotic-relevant DNA

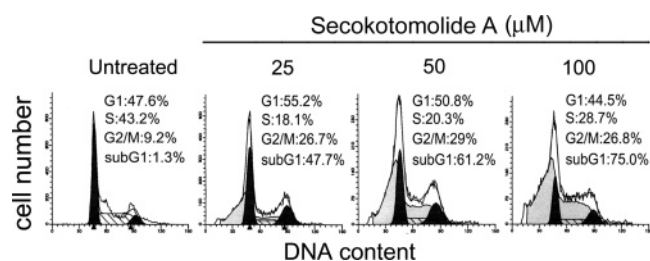


**Figure 1.** Effect of compound **4** on cell cycle of HeLa cell line. HeLa cells were treated with the indicated concentrations of **4** for 24 h. After treatment, cells were collected, fixed with MeOH, stained with propidium iodide, and analyzed by flow cytometry. Data on each sample represent the percentage of cells in the G1, S, G2M, and subG1 phases of the cell cycle, respectively. These experiments were performed at least three times, and a representative experiment is presented.

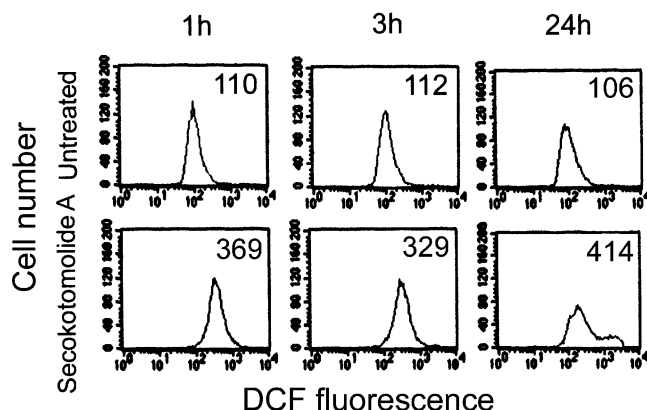


**Figure 2.** Effect of compound **4** on intracellular  $\text{H}_2\text{O}_2$  and/or peroxide of HeLa cell line. HeLa cells were treated with 100  $\mu\text{M}$  **4** for 1, 3, and 24 h. After treatment, cells were treated with 10  $\mu\text{M}$  DCFH-DA for 30 min in the dark, washed once with PBS, detached by trypsinization, collected by centrifugation, and suspended in PBS. The intracellular  $\text{H}_2\text{O}_2$  and/or peroxide, as indicated by the fluorescence of dichlorofluorescein (DCF), was measured with a Becton-Dickinson FACS-Calibur flow cytometer. The data in each panel represent the DCF fluorescence intensity within the cells. These experiments were performed at least three times, and a representative experiment is presented.

damage occurred following the addition of **4** in the human HeLa cell line. The DNA content of secokotomolide A (**4**)-treated HeLa cells was determined by staining with propidium iodide (PI) and using flow cytometry. The DNA histograms and the percentages of cells in each phase of the cell cycle are shown in Figure 1. Compared with untreated HeLa cells, treatment with 25, 50, and 100  $\mu\text{M}$  **4** for 24 h resulted in a dose-responsive increase in the subG1 population, extending from 1.4 to 68.8, 75.6, and 81.8%, respectively.

Many drugs induce apoptosis through an increased intracellular reactive oxygen species (ROS). We further examined whether **4** affected the intracellular ROS, including superoxide,  $\text{H}_2\text{O}_2$ , and peroxide of HeLa cells. Thus, the production of intracellular  $\text{H}_2\text{O}_2$  and/or peroxide was determined at 1, 3, and 24 h after the addition of **4** (100  $\mu\text{M}$ ) by flow cytometry and DCFH-DA staining.<sup>27</sup> The intracellular DCF fluorescence markedly increased to 3.4-, 2.9-, and 3.9-fold as compared with untreated HeLa cells at 1, 3, and 24 h, respectively (Figure 2). On the contrary, the intracellular superoxide level in the **4**-treated HeLa cells (as determined by hydroethidine staining) did not show significant increase (Figure 3). These results suggest that the main ROS produced by **4** is  $\text{H}_2\text{O}_2$  and/or peroxide rather than superoxide.

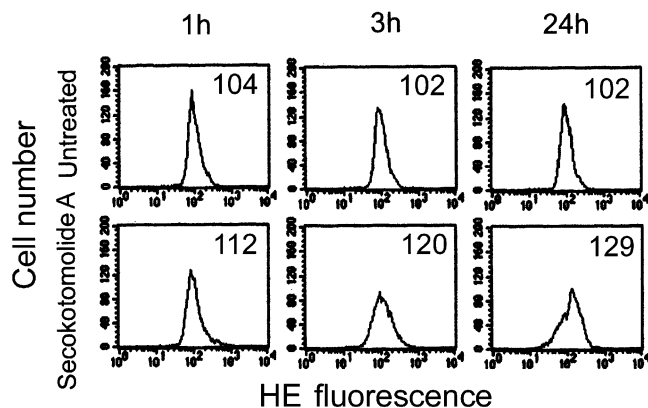


**Figure 3.** Effect of compound **4** on intracellular superoxide of HeLa cell line. HeLa cells were treated with 100  $\mu\text{M}$  **4** for 1, 3, and 24 h. After treatment, cells were treated with 10  $\mu\text{M}$  hydroethidine (HE) for 30 min in the dark, washed once with PBS, detached by trypsinization, collected by centrifugation, and suspended in PBS. The intracellular superoxide, as indicated by the fluorescence of HE, was measured with a Becton-Dickinson FACS-Calibur flow cytometer. The data in each panel represent the HE fluorescence intensity within the cells. These experiments were performed at least three times, and a representative experiment is presented.

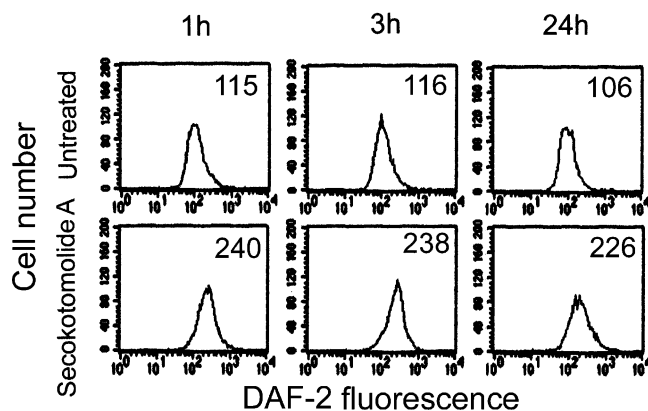


**Figure 4.** Effect of compound **4** on intracellular nitric oxide (NO) of HeLa cell line. HeLa cells were treated with 100  $\mu\text{M}$  **4** for 1, 3, and 24 h. After treatment, cells were treated with 1  $\mu\text{M}$  DAF-2 for 10 min in the dark, washed once with PBS, detached by trypsinization, collected by centrifugation, and suspended in PBS. The DAF-2 fluorescence reflecting the level of intracellular NO in cells was measured in a Becton-Dickinson FACS-Calibur flow cytometer. The data in each panel represent the DAF-2 fluorescence intensity within the cells. These experiments were performed at least three times, and a representative experiment is presented.

Some reports have demonstrated that NO has antitumor activity, and high concentrations of NO can inhibit cell growth and induce apoptosis.<sup>28,29</sup> We tested the effect of **4** on the production of intracellular NO and in HeLa cells by DAF-2 staining. Results showed that 100  $\mu\text{M}$  **4** significantly increased the DAF-2 fluorescence to 2.1-fold at every treated period, as compared with untreated cells (Figure 4). This suggests that **4** can maintain a constant increase of intracellular NO production in HeLa cells.

The cellular redox environment of GSH plays a crucial role in the progression of apoptosis.<sup>30</sup> DNA fragmentation is produced during apoptosis or necrosis induced by GSH depletion in several types of mammalian cells.<sup>31</sup> We further evaluated the intracellular GSH level by CMF-DA staining, a GSH-specific probe, and flow cytometry.<sup>27</sup> As shown in Figure 5, 25  $\mu\text{M}$  **4** could induce a 49%

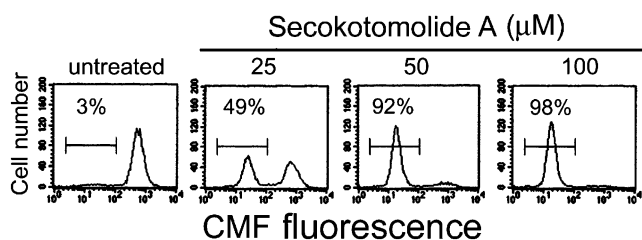


**Figure 5.** Effect of compound **4** on intracellular glutathione (GSH) of HeLa cell line. HeLa cells were treated with 25, 50, and 100  $\mu\text{M}$  **4** for 24 h. After treatment, cells were treated with 25  $\mu\text{M}$  CMF-DA for 30 min in the dark, then washed once with PBS, detached by trypsinization, collected by centrifugation, and suspended in PBS. The fluorescence mean intensity was measured by flow cytometry analysis. Data in each panel represent the percentage of cell numbers displaying intracellular GSH negative cells. These experiments were performed at least three times, and a representative experiment is presented.

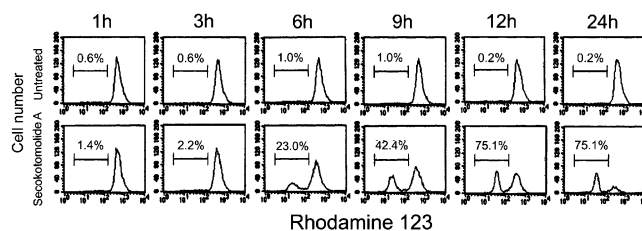


**Figure 6.** Effect of compound **4** on mitochondrial transmembrane potential ( $\Delta\Psi_m$ ) of HeLa cell line. HeLa cells were treated with 100  $\mu\text{M}$  **4** for 1, 3, 6, 9, 12, and 24 h. After treatment, the culture medium was replaced with a new medium with 5  $\mu\text{M}$  rhodamine 123 for 30 min in the dark. After the incubation step, cells were harvested by trypsinization, following which  $\Delta\Psi_m$ , as indicated by the fluorescence intensity of rhodamine 123, was analyzed using a Becton-Dickinson FACS-Calibur flow cytometer. Data in each panel represent the percentage of cell numbers displaying a decreased  $\Delta\Psi_m$ . These experiments were performed at least three times, and a representative experiment is presented.

GSH-depleted cell population as compared with untreated cells (3%) at 24 h. Notably, with the treatment of **4** at the levels of 50 and 100  $\mu\text{M}$ , the percentage of GSH-depleted cells drastically increased to 92 and 98%, respectively.

A decrease in mitochondrial transmembrane potential ( $\Delta\Psi_m$ ) has been reported as an early event in apoptosis.<sup>32</sup> To measure changes in the  $\Delta\Psi_m$ , HeLa cells treated with 100  $\mu\text{M}$  **4** and untreated HeLa cells were stained with 5  $\mu\text{M}$  rhodamine 123, a fluorescent dye reflecting  $\Delta\Psi_m$ ,<sup>33</sup> at different times after treatment with **4**. Reduced  $\Delta\Psi_m$  is reflected here in reduced staining with rhodamine 123. The percentage of cells staining weakly with rhodamine 123 in untreated cells was less than 1.0% during 1–24 h (Figure 6). On the other hand, HeLa cells treated with 100  $\mu\text{M}$  **4** showed markedly weaker staining, reflecting the loss of  $\Delta\Psi_m$ . The percentage of cells staining weakly with rhodamine 123 was 23.0, 42.4, and 75.1% at 6, 9, and 12 h, respectively. The percentage of cells staining weakly with rhodamine 123 was maintained at 75.1% after HeLa cells received **4** at 24 h.

Caspases are cysteine proteases that have a main role in apoptosis.<sup>34,35</sup> To evaluate the role played by caspases in the apoptotic effect induced by **4** (100  $\mu\text{M}$ ) in HeLa cells, the caspase 3/7 activities were examined after 3, 6, 9, 12, and 24 h of treatment. Caspase 3/7 activities of the **4**-treated cells increased about 3.5- and 5.9-fold at 3 and 6 h of treatment, respectively (Figure 7). In particular, after treatment with 100  $\mu\text{M}$  **4** as compared to untreated cells, HeLa cell populations were enhanced 9.9-fold, the largest level at 9 h in caspase 3/7 activities. The activation of caspase 3/7

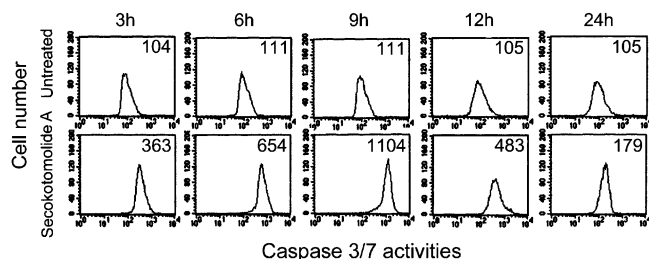


**Figure 7.** Effect of compound **4** on caspase 3/7 activities of HeLa cell line. HeLa cells were treated with 100  $\mu\text{M}$  **4** for 3, 6, 9, 12, and 24 h. After treatment, the cells were washed once with PBS, detached by trypsinization, and collected by centrifugation. Aliquots of  $1 \times 10^6$  cells were suspended in a DMEM medium, then a homogeneous substrate reagent, Z-DEVD-R110, for caspase 3/7 was added to the cells, maintaining a 1:1 ratio of reagent to cell solution. After 1 h of incubation at 37  $^{\circ}\text{C}$ , the cells were washed once with PBS, collected by centrifugation, and suspended in PBS. The substrate cleavage to release free R110 fluorescence intensity in cells was analyzed using a Becton-Dickinson FACS-Calibur flow cytometer. The data in each panel represent the R110 fluorescence intensity within the cells. These experiments were performed at least three times, and a representative experiment is presented.

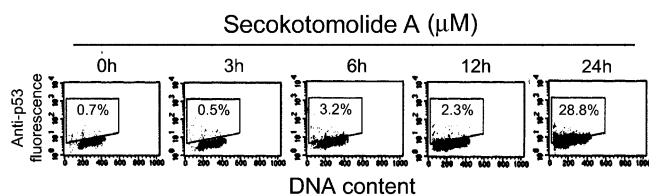


**Figure 8.** Effect of compound **4** on p53 expression of HeLa cell line. HeLa cells were treated with 100  $\mu\text{M}$  **4** for 0, 3, 6, 12, and 24 h. After treatment, both floating and adherent cells were harvested and fixed using 1% paraformaldehyde for 15 min at 4  $^{\circ}\text{C}$ . After fixation, cells were permeated with 70% EtOH for 30 min at 4  $^{\circ}\text{C}$ , followed by two washes with phosphate-buffered saline (PBS) containing 0.2% BSA. To evaluate the p53 expression,  $(1-2) \times 10^6$  cells were incubated with 20  $\mu\text{L}$  of FITC-conjugated mouse anti-p53 monoclonal antibody for 1 h at 37  $^{\circ}\text{C}$  in a humidified 5%  $\text{CO}_2$ -in-air atmosphere. After antibody incubation, cells were washed twice with PBS, suspended in PBS containing 50  $\mu\text{g}/\text{mL}$  PI and 50  $\mu\text{g}/\text{mL}$  DNase-free RNase A for 30 min at room temperature in the dark, and then analyzed by a Becton-Dickinson FACS-Calibur flow cytometer. The data in each panel represent the percentage of p53-positive cells. These experiments were performed at least three times, and a representative experiment is presented.

remained greater than untreated cells at 12 and 24 h, as it exhibited 4.6- and 1.7-fold increases, respectively.

It has been suggested that the p53 protein expression is a critical factor in the apoptosis pathway.<sup>36,37</sup> Many anticancer drugs also induced apoptosis on cancer cells through increasing p53 expression.<sup>38</sup> To determine whether the induction of apoptosis by **4** is related to p53, the expression of p53 was examined by an FITC-conjugated p53 antibody and flow cytometry analysis. Results demonstrated that the percentage of p53-positive cells was enhanced to 28.8% for HeLa cells after exposure to 100  $\mu\text{M}$  **4** at 24 h (Figure 8).

To investigate the critical event on **4**-induced apoptosis, glutathione ethyl ester (GSHEE), an intracellular GSH supplement,<sup>39</sup> Boc-Asp(OMe)-fmk, a broad caspases inhibitor,<sup>40</sup> cyclosporin A, a mitochondrial permeability transition opening inhibitor,<sup>41</sup> dexamethasone, an NO inhibitor,<sup>42</sup> and pifithrin- $\alpha$ , a p53 inhibitor,<sup>43</sup> were pretreated for 2 h and applied in **4**-induced apoptosis and analyzed by TUNEL assay and cell cycle analysis. As shown in

Figure 9A, the percentage of apoptotic cells in the untreated cells was 1.8%, and this increased to 72.3% at 24 h in the 100  $\mu\text{M}$  **4**-treated cells. The percentage of apoptosis was markedly decreased to 5.4% by 10 mM GSHEE pretreatment. Pretreatment with 100  $\mu\text{M}$  Boc-Asp(OMe)-fmk resulted in 39.0% apoptotic cells. In contrast, the percentages of apoptotic cells were 54.5, 55.3, and 57.3% in 5  $\mu\text{M}$  cyclosporin A-pretreated, 10  $\mu\text{M}$  dexamethasone-pretreated, and 10  $\mu\text{M}$  pifithrin- $\alpha$ -pretreated cells, respectively. In the cell cycle analysis, pretreatment with GSHEE also extremely decreased the percentage of sub G1, 11.3% as compared with 72.3% in cells treated with only **4**. The sub G1 in Boc-Asp(OMe)-fmk-, cyclosporin A-, dexamethasone-, and pifithrin- $\alpha$ -pretreated cells was 74.8, 61.2, 47.7, and 40.9%, respectively.

In this report, we have demonstrated that **4** potently induced apoptosis in HeLa cells with the generation of  $\text{H}_2\text{O}_2$ , peroxide, and NO, a GSH depletion, a decrease of  $\Delta\Psi_m$ , and activation of caspase 3/7 and p53 overexpression. Several studies have demonstrated that ROS induces apoptosis in several cancer cell lines.<sup>44,45</sup> Many drugs also show an anticancer effect by way of an increase in intracellular ROS.<sup>46-51</sup> These results illustrate that **4** increased about 3.4-fold for intracellular  $\text{H}_2\text{O}_2$  and/or peroxide, as compared with untreated cells in an early 1 h period of treatment. The overproduction of intracellular  $\text{H}_2\text{O}_2$  and/or peroxide was still significant even 24 h post-treatment. We suppose  $\text{H}_2\text{O}_2$  and/or peroxide increase induced by **4** triggers a series of apoptotic events, including GSH depletion, mitochondrial dysfunction, caspase 3/7 activation, and p53 overexpression in later treated periods.

Several studies have demonstrated that intracellular GSH depletion is a critical event for the initiation of DNA damage in some cancer cell lines.<sup>31,52-55</sup> In our studies, we found that **4**-treated HeLa cells produced large amounts of GSH-depleted cells (Figure 5). These data also correlate excellently with the results of **4**-mediated increase in disruption of  $\Delta\Psi_m$  and are consistent with the notion that GSH depletion could induce mitochondrial dysfunction.<sup>56,57</sup> Our present studies demonstrated that the apoptotic effect of **4** was obvious blocked by GSHEE (Figure 9). We suggest that the increased intracellular GSH depletion is a critical event in **4**-induced apoptosis in HeLa cells. As to how the underlying mechanism of **4** triggers the occurrence of GSH depletion awaits further investigation.

## Experimental Section

**General Experimental Procedures.** Optical rotations were measured with a JASCO DIP-370 digital polarimeter. UV spectra were obtained in MeCN using a JASCO V-530 spectrophotometer. Melting points were determined using a Yanagimoto micro-melting point apparatus and are uncorrected. The IR spectra were measured on a Hitachi 260-30 spectrophotometer.  $^1\text{H}$  (500 MHz, using  $\text{CDCl}_3$  or acetone- $d_6$  as solvents for measurement),  $^{13}\text{C}$  (125 MHz), DEPT, HETCOR, COSY, NOESY, and HMBC NMR spectra were obtained on a Unity Plus Varian NMR spectrometer. LRFABMS and LREIMS spectra were obtained with a JEOL JMS-SX/SX 102A mass spectrometer or a Quattro GC-MS spectrometer with a direct inlet system. HRFABMS and HREIMS were measured on a JEOL JMS-HX 110 mass spectrometer. Silica gel 60 (Merck, 230-400 mesh) was used for column chromatography. Precoated silica gel plates (Merck, Kieselgel 60 F-254, 0.20 mm) were used for analytical TLC, and precoated silica gel plates (Merck, Kieselgel 60 F-254, 0.50 mm) were used for preparative TLC. Spots were detected by spraying with 50%  $\text{H}_2\text{SO}_4$  and then heating on a hot plate. Flow cytometry analysis was done by a Becton-Dickinson FACS-Calibur flow cytometer. Labeling dyes such as propidium iodide (PI) and rhodamine 123 were used to investigate the events involved in apoptosis.

**Plant Material.** The leaves of *C. kotoense* were collected from Fooyin University, Kaohsiung County, Taiwan, in May 2004. A voucher specimen was characterized by Dr. Pei-Fang Lee of the

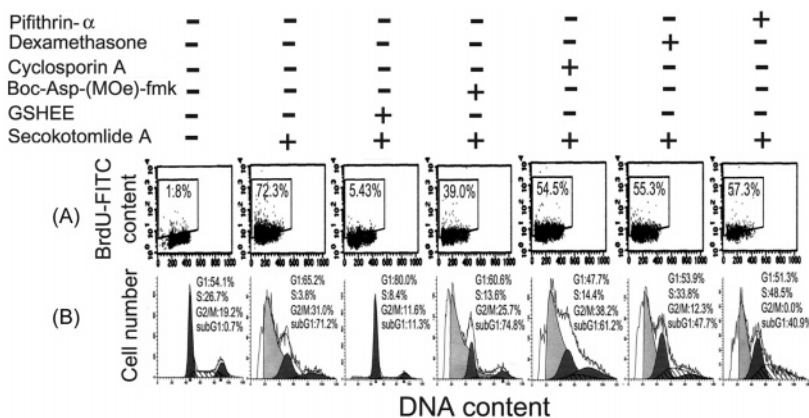


**Figure 9.** Evaluation of the critical role in **4**-induced apoptosis. HeLa cells were cultured in 60 mm tissue-culture dishes. The culture medium was replaced with a new medium when the cells were 80% confluent. HeLa cells were untreated and then treated with 100  $\mu$ M **4** alone for 24 h, pretreated with 10  $\mu$ M pifithrin- $\alpha$ , 10  $\mu$ M dexamethasone, 5  $\mu$ M cyclosporin A, 100  $\mu$ M Boc-Asp(Ome)-fmk, and 10 mM glutathione ethyl ester (GSHEE) for 1 h, exposed to 100  $\mu$ M **4** for 24 h, and then proceeded to the (A) TUNEL assay or (B) cell cycle analysis. In the TUNEL assay, the representative plots depict DNA content on the *x*-axis and BrdU-FITC-labeled apoptotic DNA strand breaks on the *y*-axis. Data represent the percentage of apoptotic cells in the upper box. These experiments were performed at least three times, and a representative experiment is presented.

Graduate Institute of Biotechnology, Fooyin University, Kaohsiung County, Taiwan, and deposited in the Basic Medical Science Education Center, Fooyin University, Kaohsiung County, Taiwan.

**Extraction and Isolation.** The air-dried leaves of *C. kotoense* (11.0 kg) were extracted with MeOH (80 L  $\times$  6) at room temperature, and the MeOH extract (201.2 g) was obtained upon concentration under reduced pressure. The MeOH extract, suspended in H<sub>2</sub>O (1 L), was partitioned with CHCl<sub>3</sub> (2 L  $\times$  5) to give fractions soluble in CHCl<sub>3</sub> (112.4 g) and H<sub>2</sub>O (56.8 g). The CHCl<sub>3</sub>-soluble fraction (112.4 g) was chromatographed over silica gel (800 g, 70–230 mesh) using *n*-hexane–EtOAc–acetone as eluent to produce five fractions. Part of fraction 1 (5.31 g) was subjected to Si gel chromatography by eluting with *n*-hexane–EtOAc (20:1), then enriched with EtOAc to furnish 10 fractions (1-1–1-10). Fraction 1-1 (1.84 g) was re-subjected to Si gel chromatography, eluting with *n*-hexane–EtOAc (50:1) and enriched gradually with EtOAc to obtain five fractions (1-1-1–1-5). Fraction 1-1-1 (0.36 g) was further purified by another silica gel column using *n*-hexane–EtOAc to obtain stearic acid (35 mg) and palmitic acid (46 mg). Fraction 1-1-2 (0.53 g) eluted with *n*-hexane–EtOAc (30:1) was further separated using silica gel CC and preparative TLC (*n*-hexane–EtOAc (30:1)), giving kotomolide B (**3**) (12 mg) and secokotomolide A (**4**) (327 mg). Fractions 1-1-3 (0.12 g) and 1-1-4 (0.24 g) were re-subjected to Si gel CC and purified by preparative TLC to yield vanillin (12 mg) and vanillic acid (6 mg). Fraction 1-4 (3.12 g) was re-subjected to Si gel chromatography, eluting with *n*-hexane–EtOAc (40:1) and enriched gradually with EtOAc, to obtain three fractions (1-4-1–1-4-3). Fraction 1-4-2 (3.01 g), eluted with *n*-hexane–EtOAc (40:1), was further separated using silica gel CC and preparative TLC (*n*-hexane–EtOAc (30:1)) and gave isobutylsilactone A (2.88 g) and obtusilactone A (121 mg). Part of fraction 2 (8.76 g) was subjected to Si gel chromatography by eluting with *n*-hexane–EtOAc (10:1), then enriched with EtOAc to furnish six fractions (2-1–2-6). Fraction 2-1 (1.24 g) was re-subjected to Si gel chromatography, eluting with CHCl<sub>3</sub>–MeOH (100:1) and enriched gradually with MeOH, to obtain 10 fractions (2-1-1–2-1-10). Fraction 2-1-2 (0.18 g) and fraction 2-1-3 (0.25 g) were re-subjected to Si gel CC and purified by preparative TLC to yield ferulic acid (7 mg), *p*-hydroxybenzaldehyde (5 mg), and syringaldehyde (11 mg). Fraction 2-3 (1.54 g) was re-subjected to Si gel chromatography, eluting with *n*-hexane–EtOAc (40:1) and enriched gradually with EtOAc, to obtain four fractions (2-3-1–2-3-4). Fraction 2-3-2 (1.06 g) eluted with *n*-hexane–EtOAc (20:1) was further separated using silica gel CC and preparative TLC (*n*-hexane–EtOAc (40:1)) and gave

kotomolide A (**1**) (37 mg) and isokotomolide A (**2**) (453 mg). Fraction 2-5 (5.43 g, *n*-hexane–EtOAc (10:1)) was further purified on a silica gel column (300 g, 230–400 mesh) using CHCl<sub>3</sub>–MeOH to obtain a mixture of  $\beta$ -sitosterol and stigmasterol (2.74 g). Part of fraction 3 (5.51 g) was subjected to Si gel chromatography by eluting with *n*-hexane–EtOAc (1:1), then enriched with EtOAc, to furnish five fractions (3-1–3-5). Fraction 3-1 (2.42 g) was further purified by another silica gel column using CHCl<sub>3</sub>–MeOH to obtain eugenol (2.01 g). Fraction 3-3 (1.75 g) was further purified on a silica gel column using CHCl<sub>3</sub>–MeOH to obtain sesamin (1.04 g) and syringaresinol (21 mg). Fraction 3-4 (0.83 g) was purified on a silica gel column using CHCl<sub>3</sub>–MeOH to obtain pulviatilol (11 mg) and clemaphenol A (4 mg). Part of fraction 4 (3.38 g) was subjected to Si gel chromatography by eluting with *n*-hexane–EtOAc (1:3), then enriched with EtOAc, to furnish five fractions (4-1–4-5). Fraction 4-3 (2.41 g) was further purified on a silica gel column (150 g, 230–400 mesh) using CHCl<sub>3</sub>–MeOH to obtain (–)-catechin (46 mg), (+)-catechin (64 mg), and (–)-epicatechin (51 mg). A mixture of  $\beta$ -sitosteryl-D-glucoside and stigmasteryl-D-glucoside (233 mg) was recrystallized (MeOH) from fraction 5 to afford crystals. Known compounds have been characterized by comparison of their spectroscopic data with literature values.<sup>4–21</sup>

**Kotomolide A [(4*S*,3*Z*)-4-hydroxy-5-methylene-3-octylidene-dihydrofuran-2-one] (1):** pale yellowish liquid; [ $\alpha$ ]<sub>D</sub><sup>25</sup> –43.2 (*c* 0.023, CHCl<sub>3</sub>); UV  $\lambda_{\max}$  (MeCN, log  $\epsilon$ ) 228 (4.11) nm; IR (neat)  $\nu_{\max}$  3450 (br, OH), 1768, 1680 ( $\alpha,\beta$ -unsaturated  $\gamma$ -lactone), 1464, 1365, 1090 cm<sup>-1</sup>; <sup>1</sup>H NMR data, see Table 1; <sup>13</sup>C NMR data, see Table 2; FABMS *m/z* 225 [M + H]<sup>+</sup> (62), 211 (13), 167 (7), 149 (11), 139 (13), 125 (29), 111 (100), 97 (80), 83 (81), 69 (89); HRFABMS *m/z* 225.1473 [M + H]<sup>+</sup> (calcd for C<sub>13</sub>H<sub>21</sub>O<sub>3</sub>, 225.1491).

**Isokotomolide A [(4*S*,3*E*)-4-hydroxy-5-methylene-3-octylidene-dihydrofuran-2-one] (2):** pale yellowish liquid; [ $\alpha$ ]<sub>D</sub><sup>25</sup> –45.6 (*c* 0.75, CHCl<sub>3</sub>); UV  $\lambda_{\max}$  (MeCN, log  $\epsilon$ ) 225 (4.13) nm; IR (neat)  $\nu_{\max}$  3445 (br, OH), 1768, 1670 ( $\alpha,\beta$ -unsaturated  $\gamma$ -lactone), 1465, 1270, 1027 cm<sup>-1</sup>; <sup>1</sup>H NMR data, see Table 1; <sup>13</sup>C NMR data, see Table 2; FABMS *m/z* 225 [M + H]<sup>+</sup> (60), 211 (14), 167 (9), 149 (23), 139 (11), 125 (32), 111 (100), 97 (77), 83 (83), 69 (93); HRFABMS *m/z* 225.1485 [M + H]<sup>+</sup> (calcd for C<sub>13</sub>H<sub>21</sub>O<sub>3</sub>, 225.1491).

**Kotomolide B [3-(1-methoxynonadecyl)-5-methylene-5H-furan-2-one] (3):** colorless oil; [ $\alpha$ ]<sub>D</sub><sup>25</sup> –47.6 (*c* 0.04, CHCl<sub>3</sub>); UV  $\lambda_{\max}$  (MeCN, log  $\epsilon$ ) 265 (4.07) nm; IR (neat)  $\nu_{\max}$  3455 (br, OH), 1780, 1680 ( $\alpha,\beta$ -unsaturated  $\gamma$ -lactone), 1290 cm<sup>-1</sup>; <sup>1</sup>H NMR (500 MHz, CDCl<sub>3</sub>)  $\delta$  0.87 (3H, t, *J* = 6.8 Hz, H-19'), 1.26 (30H, br s, H-4'–18'), 1.42–1.68 (4H, m, H-2', 3'), 3.35 (3H, s, OMe-1'), 4.12 (1H, dd, *J* = 7.4, 4.8 Hz, H-1'), 4.88, 5.20 (each 1H, d, *J* = 2.6

Hz, H-6a, b), 7.22 (1H, br s, H-4);  $^{13}\text{C}$  NMR (125 MHz,  $\text{CDCl}_3$ )  $\delta$  14.3 (C-19'), 22.7 (C-18'), 25.5 (C-3'), 29.0–30.0 (C-4'–16'), 31.8 (C-17'), 35.2 (C-2'), 57.5 (OMe-1'), 77.3 (C-1'), 97.9 (C-6), 137.7 (C-4), 137.8 (C-3), 155.1 (C-5), 169.8 (C-2); EIMS  $m/z$  392  $[\text{M}]^+$  (1), 280 (8), 267 (5), 179 (7), 165 (13), 149 (14), 142 (100), 123 (24), 111 (31), 97 (45), 83 (41), 69 (74), 55 (92); HREIMS  $m/z$  392.3277  $[\text{M}]^+$  (calcd for  $\text{C}_{25}\text{H}_{44}\text{O}_3$ , 392.3290).

**Secokotomolide A** {methyl[(2E)-2-[(1R)-1-hydroxy-2-oxopropyl]hexadec-2-enoate]} (**4**): pale yellowish liquid;  $[\alpha]_D^{25}$   $-52.1$  ( $c$  0.15,  $\text{CHCl}_3$ ); UV  $\lambda_{\text{max}}$  (MeCN,  $\log \epsilon$ ) 215 (3.79) nm; IR (neat)  $\nu_{\text{max}}$  3450 (br, OH), 1735 (ester), 1710 (ketone)  $\text{cm}^{-1}$ ;  $^1\text{H}$  NMR (500 MHz, acetone- $d_6$ )  $\delta$  0.88 (3H, t,  $J = 6.8$  Hz, H-16), 1.28 (20H, br s, H-6~15), 1.47 (2H, m, H-5), 2.12 (3H, s, H-3'), 2.34 (2H, q,  $J = 7.4$  Hz, H-4), 3.65 (3H, s, OMe-1), 4.08 (1H, br d,  $J = 3.2$  Hz, OH-1',  $\text{D}_2\text{O}$  exchangeable), 4.78 (1H, br d,  $J = 3.2$  Hz, H-1'), 6.98 (1H, t,  $J = 7.6$  Hz, H-3);  $^{13}\text{C}$  NMR (125 MHz, acetone- $d_6$ )  $\delta$  14.1 (C-16), 22.6 (C-15), 24.5 (C-3'), 28.6 (C-4), 28.7 (C-5), 29.0–30.0 (C-6–13), 31.9 (C-14), 52.1 (OMe-1), 74.1 (C-1'), 129.5 (C-2), 149.4 (C-3), 166.5 (C-1), 206.3 (C-2'); FABMS  $m/z$  341  $[\text{M} + \text{H}]^+$  (2), 323 (1), 309 (6), 297 (69), 265 (74), 247 (8), 237 (12), 219 (18), 191 (9), 167 (10), 155 (16), 149 (23), 125 (41), 115 (78), 97 (81), 83 (97), 69 (92), 55 (100); HRFABMS  $m/z$  341.2689  $[\text{M} + \text{H}]^+$  (calcd for  $\text{C}_{20}\text{H}_{37}\text{O}_4$ , 341.2692).

**Cell Culture and Drug Treatments.** HeLa cells were seeded into 60 mm tissue culture dishes ( $5 \times 10^5$  cells/dish) 48 h before the experiment. The basal medium was Dulbecco's modified Eagle's medium (DMEM) supplemented with 10% FCS, 100 units/mL penicillin G, 100  $\mu\text{g}/\text{mL}$  streptomycin, and 250  $\mu\text{g}/\text{mL}$  amphotericin B. The stock solution of compound **4** (100 mM) was dissolved in DMSO, and experimental concentrations were prepared in the basal medium. The final concentration of DMSO in the medium was 0.1%. Cells were exposed to medium containing various concentrations of **4** for different periods.

**Propidium Iodide (PI) Staining of Cellular DNA.** After drug treatment, adherent and floating HeLa cells were pooled, washed with PBS, fixed in PBS–MeOH (1:2, v/v) solution, and maintained at 4 °C for at least 18 h. After an additional wash with PBS, the cell pellets were stained with the fluorescent probe solution containing PBS, 50  $\mu\text{g}$  of propidium iodide/mL, and 50  $\mu\text{g}$  of DNase-free RNaseA/mL for 30 min at room temperature in the dark. Cells were then analyzed using a FACS-Calibur cytometer (Becton Dickinson, San Jose, CA) with excitation at 488 nm, and gating out of doublets and clumps using pulse processing and collection of fluorescence emission above 580 nm. The percentage of cells undergoing DNA damage was defined as the percentage of cells in the subdiploid region (subG1) of the DNA distribution histograms.

**Analysis of Intracellular  $\text{H}_2\text{O}_2$  and/or Peroxide by Flow Cytometry.** Production of intracellular  $\text{H}_2\text{O}_2$  and/or peroxide was detected by flow cytometry using 2',7'-dichlorodihydrofluorescein diacetate (DCFH-DA).<sup>27</sup> Cells were cultured in 60 mm tissue-culture dishes. The culture medium was replaced with new medium when the cells were 80% confluent and then exposed to 100  $\mu\text{M}$  **4** for 1, 3, and 24 h. After drug treatment, cells were treated with 10  $\mu\text{M}$  DCFH-DA for 30 min in the dark, washed once with PBS, detached by trypsinization, collected by centrifugation, and suspended in PBS. The intracellular  $\text{H}_2\text{O}_2$  and/or peroxide, as indicated by the fluorescence of dichlorofluorescein (DCF), was measured with a Becton-Dickinson FACS-Calibur flow cytometer.

**Analysis of Intracellular Superoxide by Flow Cytometry.** Production of intracellular superoxide was detected by flow cytometry using hydroethidine (HE). Cells were cultured in 60 mm tissue-culture dishes. The culture medium was replaced with new medium when the cells were 80% confluent and then exposed to 100  $\mu\text{M}$  **4** for 1, 3, and 24 h. After drug treatment, cells were treated with 10  $\mu\text{M}$  HE for 30 min in the dark, washed once with PBS, detached by trypsinization, collected by centrifugation, and sus-

ended in PBS. The intracellular superoxide, as indicated by the fluorescence of HE, was measured with a Becton-Dickinson FACS-Calibur flow cytometer.

**Analysis of Intracellular NO by Flow Cytometry.** Production of intracellular NO was detected by flow cytometry using 4,5-diaminofluorescein (DAF-2). Cells were cultured in 60 mm tissue-culture dishes. The culture medium was replaced with new medium when the cells were 80% confluent and then exposed to 100  $\mu\text{M}$  **4** for 1, 3, and 24 h. After drug treatment, cells were treated with 1  $\mu\text{M}$  DAF-2 for 10 min in the dark, washed once with PBS, detached by trypsinization, collected by centrifugation, and suspended in PBS. The DAF-2 fluorescence reflecting the level of intracellular NO in cells was measured in a Becton-Dickinson FACS-Calibur flow cytometer.

**Analysis of Intracellular GSH Content by Flow Cytometry.** The level of intracellular GSH per cell was determined by flow cytometry after staining with chloromethylfluorescein diacetate (CMF-DA).<sup>27</sup> Cells were cultured in 60-mm tissue-culture dishes. The culture medium was replaced with new medium when the cells were 80% confluent and then exposed to 25, 50, and 100  $\mu\text{M}$  **4** for 24 h. After drug treatment, adherent and floating HeLa cells were pooled and washed with PBS. The CMF-DA was added at 25  $\mu\text{M}$  in cell suspensions adjusted at  $(1-2) \times 10^6$  cells per mL. After 30 min of incubation at 37 °C, cells were washed twice in PBS, resuspended at a concentration of  $10^6$  cells/mL in PBS, and analyzed on a Becton-Dickinson FACS-Calibur flow cytometer.

**Analysis of  $\Delta\Psi_m$  by Flow Cytometry.** The  $\Delta\Psi_m$  per cell was determined by flow cytometry after staining with rhodamine 123.<sup>33</sup> Rhodamine 123 is a fluorescent dye that is incorporated into mitochondria in a transmembrane potential-dependent manner. Cells were cultured in 60 mm tissue-culture dishes. The culture medium was replaced with new medium when the cells were 80% confluent and then exposed to 100  $\mu\text{M}$  **4** for 1, 3, 6, 9, 12, and 24 h. After drug treatment, cells were treated with 5  $\mu\text{M}$  rhodamine 123 for 30 min in the dark, washed once with PBS, detached by trypsinization, collected by centrifugation, and suspended in PBS. The  $\Delta\Psi_m$  determined by the fluorescence level of rhodamine 123 was analyzed using a Becton-Dickinson FACS-Calibur flow cytometer.

**Analysis of Caspase 3/7 Activities by Flow Cytometry.** Caspase 3/7 activities were measured by a method modified from an experienced user's protocol on the Apo-one homogeneous caspase-3/7 assay kit. The Z-DEVD-R110 substrate for caspase 3/7 was diluted with a buffer to make the desired amount of homogeneous substrate reagent. Cells were cultured in 60 mm tissue-culture dishes. The culture medium was replaced with a new medium when the cells were 80% confluent and then treated with 100  $\mu\text{M}$  **4** for 3, 6, 9, 12, and 24 h. After drug treatment, the cells were washed once with PBS, detached by trypsinization, and collected by centrifugation. An aliquot of  $1 \times 10^6$  cells was suspended in DMEM medium, then Z-DEVD-R110 substrate reagent was added, maintaining a 1:1 ratio of reagent to cell solution. After 1 h of incubation at 37 °C, the cells were washed once with PBS, collected by centrifugation, and suspended in PBS. Substrate cleavage to release free R110 fluorescence intensity representing the caspase-3/7 activities was measured in a Becton-Dickinson FACS-Calibur flow cytometer with excitation wavelength set at 488 nm and emission wavelength at 520 nm.

**Analysis of p53 Expression by Flow Cytometry.** Cells were cultured in 60 mm tissue-culture dishes. The culture medium was replaced with new medium when the cells were 60% confluent and then exposed to 100  $\mu\text{M}$  **4** for 0, 3, 6, 12, and 24 h. After treatment with **4**, both floating and adherent cells were harvested and fixed using 1% paraformaldehyde for 15 min at 4 °C. After fixation, cells were permeated with 70% EtOH for 30 min at 4 °C, followed by two washes with phosphate-buffered saline (PBS) containing 0.2% BSA. To evaluate the p53 expression,  $(1-2) \times 10^6$  cells were incubated with 20  $\mu\text{L}$  of FITC-conjugated mouse anti-p53 mono-

clonal antibody for 1 h at 37 °C in a humidified 5% CO<sub>2</sub>-in-air atmosphere. After antibody incubation, cells were washed twice with PBS, suspended in PBS containing 50 µg/mL PI and 50 µg/mL DNase-free RNase A for 30 min at room temperature in the dark, and then analyzed by a Becton-Dickinson FACS-Calibur flow cytometer.

**TUNEL Assay for Apoptosis.** Following incubation with various drugs, TUNEL was performed using the "Apo-BrdU" kits (BD Pharmingen, San Diego, CA), with the standard protocol provided by the manufacturer being used. Both floating and adherent cells were harvested and fixed using 1% paraformaldehyde for 30 min at 4 °C. After fixation, cells were permeated with 70% EtOH for 30 min at -20 °C, followed by two washes with phosphate-buffered saline (PBS) containing 0.2% BSA. To label DNA strand breaks, (1-2) × 10<sup>6</sup> cells were incubated with 50 µL of TUNEL reaction buffer containing terminal deoxynucleotidyl transferase and fluorescein-BrdUTP, then incubated for 1 h at 37 °C in a humidified 5% CO<sub>2</sub>-in-air atmosphere. Cells were washed twice with PBS, suspended in PBS containing 40 µg/mL PI and 40 µg/mL DNase-free RNase A for 30 min at room temperature in the dark, and then analyzed by a Becton-Dickinson FACS-Calibur flow cytometer.

**Acknowledgment.** This investigation was supported by a grant from the National Science Council of the Republic of China NSC-93-2320-B-242-008 (C.-Y.C.) and NSC-94-2320-B-242-007 (C.-H.C.). The authors are also thankful to Dr. R. H. Liu for his assistance in rewording a few paragraphs.

#### References and Notes

- Liao, J. C. *Lauraceae in Flora of Taiwan*, 2nd ed.; Editorial Committee of the Flora of Taiwan: Taipei, 1996; Vol. 2, pp 443-483.
- Chen, F. C.; Peng, C. F.; Tsai, I. L.; Chen, I. S. *J. Nat. Prod.* **2005**, *68*, 1318-1323.
- Kuo, Y. C.; Lu, C. K.; Huang, L. W.; Kuo, Y. H.; Chang, C.; Hsu, F. L.; Lee, T. H. *Planta Med.* **2005**, *71*, 412-415.
- Kwon, H. C.; Baek, N. I.; Choi, S. U.; Lee, K. R. *Chem. Pharm. Bull.* **2000**, *48*, 614-616.
- Morimoto, S.; Nonaka, G.; Nishioka, I.; Ezaki, N.; Takizawa, N. *Chem. Pharm. Bull.* **1985**, *33*, 2281-2286.
- Zhang, H. L.; Nagatsu, A.; Okuyama, H.; Mizukami, H.; Sakakibara, J. *Phytochemistry* **1998**, *48*, 665-668.
- Lee, S. S.; Wang, J. W.; Chen, K. C. S. *J. Chin. Chem. Soc.* **1995**, *42*, 77-82.
- Sun, N. J.; Chang, C. J.; Cassady, J. M. *Phytochemistry* **1987**, *26*, 3051-3053.
- Chen, C. Y.; Wu, T. Y.; Chang, F. R.; Wu, Y. C. *J. Chin. Chem. Soc.* **1998**, *45*, 629-634.
- Koul, S. K.; Taneja, S. C.; Agarwal, V. K.; Dhar, K. L. *Phytochemistry* **1988**, *27*, 3523-3527.
- He, M.; Zhang, J.; Hu, C. J. *Chin. Pharm. Sci.* **2001**, *10*, 180-182.
- Chen, L. H.; Kuo, Y. H. *J. Chin. Chem. Soc.* **1985**, *32*, 169-172.
- Chen, C. Y.; Chang, F. R.; Teng, C. M.; Wu, Y. C. *J. Chin. Chem. Soc.* **1999**, *46*, 77-86.
- Cardona, L.; Garcia, B.; Pedro, J. R.; Perez, J. *Phytochemistry* **1992**, *31*, 3989-3994.
- Kang, S. S.; Chang, Y. S.; Kim, J. S. *Chem. Pharm. Bull.* **2000**, *48*, 1242-1245.
- Tsai, I. L.; Jeng, Y. F.; Duh, C. Y.; Chen, I. S. *Chin. Pharm. J.* **2001**, *53*, 291-301.
- Ren, X. F.; Chen, X. C.; Peng, K.; Xie, X.; Xia, Y.; Pan, X. F. *Tetrahedron Asymmetry* **2002**, *13*, 1799-1804.
- Kojima, H.; Sato, N.; Hatana, A.; Ogura, H. *Phytochemistry* **1990**, *29*, 2351-2355.
- Li, J.; Kadota, S.; Kawada, Y.; Hattori, M.; Xu, G. J.; Namba, T. *Chem. Pharm. Bull.* **1992**, *40*, 3133-3137.
- Addae-Mensah, I.; Achenbach, H. *Phytochemistry* **1985**, *24*, 1817-1819.
- Dupont, M. P.; Llabres, G.; Delaude, C.; Tchissambou, L.; Gastmans, J. P. *Planta Med.* **1997**, *63*, 282-284.
- Cheng, M. J.; Tsai, I. L.; Lee, S. J.; Jayaprakasam, B.; Chen, I. S. *Phytochemistry* **2005**, *66*, 1180-1185.
- Martinez, J. C.; Yoshida, M.; Gottlieb, O. R. *Phytochemistry* **1981**, *20*, 459-464.
- Anderson, J. E.; Ma, W.; Smith, D. L.; Chang, C. J.; McLaughlin, J. L. *J. Nat. Prod.* **1992**, *55*, 71-83.
- Tanaka, H.; Nakamura, T.; Ichino, K.; Ito, K. *Phytochemistry* **1989**, *28*, 1905-1907.
- Tsai, I. L.; Hung, C. H.; Duh, C. Y.; Chen, I. S. *Planta Med.* **2002**, *68*, 138-145.
- Hsieh, T. J.; Liu, T. Z.; Chia, Y. C.; Chern, C. L.; Lu, F. J.; Chuang, M. C.; Mau, S. Y.; Chen, S. H.; Syu, Y. H.; Chen, C. H. *Food Chem. Toxicol.* **2004**, *42*, 843-850.
- Wink, D. A.; Vodovotz, Y.; Laval, J.; Laval, F.; Dewhirst, M. W.; Mitchell, J. B. *Carcinogenesis* **1998**, *19*, 711-721.
- Kim, P. K.; Zamora, R.; Petrosko, P.; Billiar, T. R. *Int. Immunopharmacol.* **2001**, *1*, 1421-1441.
- Hancock, J. T.; Desikan, R.; Neill, S. J. *Ann. N. Y. Acad. Sci.* **2003**, *1010*, 446-448.
- Higuchi, Y. *J. Cell. Mol. Med.* **2004**, *8*, 455-464.
- Hengartner, M. O. *Nature* **2000**, *407*, 770-776.
- Chen, C. H.; Chern, C. L.; Lin, C. C.; Lu, F. J.; Shih, M. K.; Hsieh, P. Y.; Liu, T. Z. *Planta Med.* **2003**, *69*, 1119-1124.
- Riedl, S. J.; Shi, Y. *Nat. Rev. Mol. Cell Biol.* **2004**, *5*, 897-907.
- Takahashi, A.; Masuda, A.; Sun, M.; Centonze, V. E.; Herman, B. *Brain Res. Bull.* **2004**, *62*, 497-504.
- Schuler, M.; Green, D. R. *Trends Genet.* **2005**, *21*, 182-187.
- Attardi, L. D. *Mutat. Res.* **2005**, *569*, 145-157.
- Bykov, V. J.; Wiman, K. G. *Ann. Med.* **2003**, *35*, 458-465.
- Boyd-Kimball, D.; Sultana, R.; Abdul, H. M.; Butterfield, D. A. *J. Neurosci. Res.* **2005**, *79*, 700-706.
- Thornberry, N. A.; Lazebnik, Y. *Science* **1998**, *281*, 1312-1316.
- Whiteman, M.; Rose, P.; Siau, J. L.; Cheung, N. S.; Halliwell, B.; Armstrong, J. S. *Free Radical Biol. Med.* **2005**, *38*, 1571-1584.
- Yu, J. S.; Tsai, H. C.; Wu, C. C.; Weng, L. P.; Li, H. P.; Chung, P. J.; Chang, Y. S. *Oncogene* **2002**, *21*, 8047-8061.
- Walton, M. I.; Wilson, S. C.; Hardcastle, I. R.; Mirza, A. R.; Workman, P. *Mol. Cancer Ther.* **2005**, *4*, 1369-1377.
- Pervin, S.; Singh, R.; Freije, W. A.; Chaudhuri, G. *Cancer Res.* **2003**, *63*, 8853-8860.
- Cook, T.; Wang, Z.; Alber, S.; Liu, K.; Watkins, S. C.; Vodovotz, Y.; Billiar, T. R.; Blumberg, D. *Cancer Res.* **2004**, *64*, 8015-8021.
- Naimi, E.; Zhou, A.; Khalili, P.; Wiebe, L. I.; Balzarini, J.; De Clercq, E.; Knaus, E. E. *J. Med. Chem.* **2003**, *46*, 995-1004.
- Ravid, A.; Koren, R. *Recent Results Cancer Res.* **2003**, *164*, 357-367.
- Pelicano, H.; Carney, D.; Huang, P. *Drug Resist. Updates* **2004**, *7*, 97-110.
- Fukuzawa, K.; Kogure, K.; Morita, M.; Hama, S.; Manabe, S.; Tokumura, A. *Biochemistry* **2004**, *69*, 50-57.
- Moharram, S.; Zhou, A.; Wiebe, L. I.; Knaus, E. E. *J. Med. Chem.* **2004**, *47*, 1840-1846.
- Huang, R.; Wallqvist, A.; Covell, D. G. *Biochem. Pharmacol.* **2005**, *69*, 1009-1039.
- Schnelldorfer, T.; Gansauge, S.; Gansauge, F.; Schlosser, S.; Beger, H. G.; Nussler, A. K. *Cancer* **2000**, *89*, 1440-1447.
- Troyano, A.; Fernandez, C.; Sancho, P.; De Blas, E.; Aller, P. *J. Biol. Chem.* **2001**, *276*, 47107-47115.
- Chen, S. J.; Wang, J. L.; Chen, J. H.; Huang, R. N. *Free Radical Biol. Med.* **2002**, *33*, 464-472.
- Cuadrado, A.; Garcia-Fernandez, L. F.; Gonzalez, L.; Suarez, Y.; Losada, A.; Alcaide, V.; Martinez, T.; Fernandez-Sousa, J. M.; Sanchez-Puelles, J. M.; Munoz, A. *J. Biol. Chem.* **2003**, *278*, 241-250.
- Lee, A. U.; Farrell, G. C. *J. Hepatol.* **2001**, *35*, 756-764.
- Knight, T. R.; Jaeschke, H. *Toxicol. Appl. Pharmacol.* **2002**, *181*, 133-141.